


Article

Explaining the Mean and Variability of Extra Travel Time in Traffic with Interacting Fast and Slow Vehicles

José Gerardo Carrillo-González ^{1,2,*} and Francisco Perez-Martinez ^{2,*} 

¹ Consejo Nacional de Ciencia y Tecnología, Mexico City 03940, Mexico

² Departamento de Sistemas de Información y Comunicaciones, Universidad Autónoma Metropolitana, Lerma de Villada 52005, Mexico

* Correspondence: j.carrillo@correo.ler.uam.mx (J.G.C.-G.); f.perez@correo.ler.uam.mx (F.P.-M.)

Abstract: In this work, the authors developed procedures to explain mean extra travel time (T) and extra travel time variability (V). This was carried out for situations (through simulations) where the fast vehicles' travel time, whose speed tendency (sp_1) is the permitted speed limit, is negatively affected (i.e., increasing travel time) by the presence of slow vehicles, whose speed tendency (sp_2) is half the speed limit. The speed limit was set in the range of 60 km/h to 90 km/h, with seven cases, and every case had eight simulations, each with different p_1 (fast vehicles' percentage) and $p_2 = 100\% - p_1$ (slow vehicles' percentage) values. p_2 ranged from 10% to 80% at intervals of 10%, for a total of 56 simulations. From the simulations' data, we calculated the fast vehicles' extra travel time, which is the additional time to traverse an avenue segment owing to the presence of slow vehicles. The fast and slow vehicles recreate heterogenous traffic in terms of speed. We developed procedures for modeling T and V with p_2 , and V with T . For modeling, $\sim 71.42\%$ of the data from simulations was used. We find that the models' parameters values can be used for explaining the remaining data. In addition, we discovered that the pattern of p_2 vs. V , for p_2 ranging from 50% to 80%, is different among sp_1 cases and not linear.

Keywords: extra travel time; fast vehicles; heterogeneous speed; slow vehicles; variability



Citation: Carrillo-González, J.G.; Perez-Martinez, F. Explaining the Mean and Variability of Extra Travel Time in Traffic with Interacting Fast and Slow Vehicles. *Appl. Sci.* **2022**, *12*, 7176. <https://doi.org/10.3390/app12147176>

Academic Editor: Luís Picado Santos

Received: 26 May 2022

Accepted: 3 July 2022

Published: 16 July 2022

Publisher's Note: MDPI stays neutral with regard to jurisdictional claims in published maps and institutional affiliations.



Copyright: © 2022 by the authors. Licensee MDPI, Basel, Switzerland. This article is an open access article distributed under the terms and conditions of the Creative Commons Attribution (CC BY) license (<https://creativecommons.org/licenses/by/4.0/>).

1. Introduction

Bad traffic is experienced in most cities of developing countries. A current traffic problem, which is getting worse every day, is the increase in travel times (see the congestion levels in [1]). Thus, gaining insight into situations inducing higher travel times is of utter importance. One of those situations is when drivers, intentionally or owing to the operating limitations of the vehicle they drive, travel at a lesser speed than the posted speed limit. Therefore, in the same stretch of road, the drivers' desired speed (or speed tendency) may vary and there is a likely chance of slow vehicles impeding fast vehicles. The traffic outcome when fast and slow vehicles interact is difficult to establish and is related with the drivers' desired speed and the percentage of slow vehicles, among other variables.

The aim of the present research is, firstly, to perform simulations with different percentages of fast and slow vehicles for proposed values for each speed tendency. The output of these simulations is the mean extra travel time (T) and the extra travel time variability (V) of the fast vehicles. These data (i.e., T and V) are divided into two groups: the data for modeling and the data for validating. Later, procedures for modeling T and V are proposed with the intention to prove if the patterns in the data (for modeling) can be reproduced. In addition, we demonstrate that the data for validating can be explained with the proposed models, and we present how to calculate the models' parameter values as part of the procedures.

In a traffic scenario with vehicles driving slower than the general traffic stream (thus generating a speed differential), when the faster vehicles are impeded by the slower

vehicles, the former are tempted to perform overtaking maneuvers, if possible. In [2], it was proven that the vehicles' travel speed (and thus also travel time) is affected, among others, by the traffic composition in terms of speeds. In [3], a relationship between speed variance and accidents was established, finding that an increase in average speed does not necessarily increase accident rates, but an increase in speed variance certainly increases them. In [4], the proposed algorithm triggers a need to overtake when the speed differential is 8 km/h. The work in [5] focuses on establishing (via simulations) the average travel time to complete a highway segment and the number of passenger cars' lane changes with different percentages of heavy trucks. The results show that both variables increase as the percentage of heavy trucks increases, with the influence of heavy trucks on traffic being notorious in heavy traffic. In [6], speed indicators on sites with uniform speed limits (65 mph for passenger vehicles and trucks/buses) and with differential speed limits (70 mph for passenger vehicles and 60 mph for trucks/buses) were investigated. The results from the models were a mean speed of 65.3 mph for the uniform case (one) and 66.9 mph for the differential case (two). Similarly, the 85th percentile speed results were 70.7 mph for case one and 73.9 mph for case two. Finally, the standard deviation was 5.5 mph for case one and 6.8 mph for case two. Through simulations, the impact on traffic of differential speed controls was investigated in [7]. The speed control strategies were uniform posted speed limits (USLs), differential posted car-truck speed limits (DSLs), and differential mandated truck speed limits (MSLs). Considered positive for traffic safety, DSL and MSL reduce average travel speed, increase head-on time-to-collision, and reduce car-car overtaking. Considered negative, DSL and MSL increase percentage time spent following and total number of overtakes, decrease car-car overtaking, but increase car-truck overtaking. In [8], considering all types of vehicles, it was detected that the highest travel speed variability occur in freeways with DSL, followed by urban freeways with USL and a speed limit of 55 mph. For passenger cars, the speed was consistent when the speed limit was 70 mph, but at lower speed limits, more speed variation was detected.

Different factors are related to free-flow speed; one of those is differential speed. In [9], the free-flow speed was modeled considering as an explanatory variable the trucks' percentage in order to test if the flow heterogeneity (the traffic composition in terms of vehicles' type) impacted speed. The results showed that the trucks' percentage is significant for the four models: daytime speed for cars and trucks, and nighttime for cars and trucks. In [10], with the aim of identifying explanatory factors for mean speed and speed dispersion considering two-lane rural highways on tangent segments and horizontal curves, free-flow speed models were developed.

The drivers' travel speed is influenced by the posted speed limit. In [11], it was found that the posted speed limit is highly correlated with the average free-flow speed for urban streets, multilane highways, and freeways. In [12], the speed limits in Utah rural interstates were increased from 75 to 80 mph, finding that the travel speed and the probability to overcome the speed limit were then higher, and that by increasing the speed limit, the speed variance was not reduced. However, as the literature review presented in [13] suggests, the results concerning the effects of speed limit on speed variation do not support each other. The investigation in [14] centers on the local and global impacts of speed limits considering two groups of drivers—the compliant and the non-compliant drivers. When choosing speed, both consider the travel time cost, the perceived crash risk, and the perceived ticket risk.

The factors influencing the drivers' desired speed on the road are numerous. There are multiple interacting factors that explain drivers' behaviors [15]. A study on drivers' speeding behavior is presented in [16]. The drivers' characteristics and their relation to speed (as a risk of accidents level) are presented in [17]. In [18], the drivers' speed choice (when there is at least a 6 s time gap to the next vehicle) at two different sites were compared, and at two different days for the same site. How a driver is influenced by the collective driving behavior is discussed in [19]. Empirical evidence suggesting that the speed choice is influenced by the pleasure of driving and other drivers' behavior is presented in [20].

Preliminary data for supporting the notion that a driver adjusts their speed by comparing their own speed with that of others are introduced in [21]. A model including attitudes and perceptions of other drivers' behavior explains approximately 15% of the variation in observed speed [22]. A speed choice prediction model was presented in [23]. It was found that the number of heavy vehicles (trucks and buses) and four-wheelers (informal para-transit) flowing in the same direction as the subject vehicle negatively influences the driver speed choice of the higher-speed class, and the same applies for trucks and motorcycles driving in the opposite direction. Buses, trucks, four-wheelers, and motorcycles negatively influence the speed of the lower-speed class (same traffic direction), and the same applies for non-motorized and buses driving in the opposite direction. The operating speed was modeled in [24], and the dependence of the drivers' speed choice on individual driver' behavior and the roadway geometry was demonstrated.

The necessity of vehicle class-specific modeling has been noted. Models to establish the free-flow speed of different types of vehicles are presented in [25]. In [26], it was found that the level-of-service (LOS) is different for each vehicle type. Besides, removing some vehicle types seems suitable to improve the system performance. Further, it was noticed that, in mixed traffic, the average stream speed better represents the dominant vehicle type, which is two-wheelers in [26]. The work in [27] uses percent speed-reduction and percent slower vehicles to define the LOS of a two-lane highway under heterogeneous traffic. It was concluded that it is impractical to evaluate the LOS of the entire traffic situation (with integration of motorized and non-motorized modes) with a common scale. In [28], two new methodologies are presented for estimating the percent time spent following (PTFS) on two-lane highways. The probabilistic method considers the slow-moving vehicles' average speed and the distribution of the desired speeds to calculate the percentage of vehicles whose desired speed is superior to the slower vehicles' average speed. This percentage (used to calculate the probability of a vehicle being impeded), along with the probability of a vehicle being part of a platoon, are used to calculate the percent following (PF), which is a surrogate measure for PTFS. In [29], it was noticed that the aggregation of faster and slower vehicles on a single class may not capture the interactions among the vehicles of the same class.

The dynamic of homogeneous and heterogeneous traffic is very different; in the latter, there are different types of vehicles, thus there are interactions (such as lane change maneuvers) between slow-moving and fast-moving vehicles. In [30], particle-hopping models for two-lane traffic were developed considering two types of vehicles: fast and slow vehicles, where the fast vehicles' maximum allowed speed is considerable higher than that of the slow vehicles. The proposed models are different from each other because of the lane-changing rules, thus producing different results about the movement of the fast and slow vehicles. In [31], the heterogeneous traffic behavior in developing countries was reproduced with a discrete cellular automata (CA) model, modeling five types of vehicles: car, bus, truck, two-wheeler, and three-wheeler. In [32], a CA model was used to simulate traffic in a two-lane system; it was demonstrated that even small densities of slow vehicles induced the formation of platoons. Moreover, modifications were incorporated into the basic model, e.g., for allowing drivers to anticipate the speed of their predecessor, leading to diminishing the effect of slow vehicles. The multi-class traffic flow model presented in [33] incorporates heterogeneous drivers, i.e., drivers selecting a different speed to drive, thus there are faster vehicles trying to overtake slower vehicles. In addition, the model explains traffic flow theory phenomena: two-capacity regimes in the fundamental diagram, hysteresis, and platoon dispersion. In [34], a vehicle class was defined considering the desired speed in free-flow conditions, and a multiclass first-order simulation model was proposed that can replicate non-linear phenomena, including the dispersion of traffic platoons when a distribution of desired speeds exists. In [35], data were collected in several two-lane roads in India, and it was observed that the capacity decreases as the proportion of three-wheeler, tractor, or heavy vehicle increases, and that the capacity increases as the proportion of two-wheeler increases. In [36], through agent-based modeling, simulations

representative of the traffic in the USA (with cars and trucks) and of the traffic in India (with different types of vehicles) were performed. It was found that the heterogeneity of vehicle types causes a high number of lane changes.

In this investigation, we simulate and analyze traffic, where the speed differential affects travel speed, thus affecting travel time. We were interested in finding a relation between the percentage of slow vehicles and two variables related with the fast vehicles: the mean extra travel time (T) and the extra travel time variability (V). We propose procedures for modeling two metrics of importance in traffic studies: T and V , which were calculated with the fast vehicles' travel times from simulations. Our research is different from the current literature as we perform traffic simulations considering a wide range of fast and slow vehicles' percentage values for a wide range of fast and slow vehicles' speed tendency values, thus adding insight for this kind of traffic situation. Our proposed procedures have the advantage of including a method for calculating the parameters' values of the models that describe the data (T and V) that were not used to calibrate the models. In this research, we have two general objectives:

- (1) For each fast vehicles' speed tendency (sp_1) value, to run a simulation for each slow vehicles' percentage (p_2) value, in order to acquire traffic information (the fast vehicles' travel times) and calculate the mean extra travel time and the extra travel time variability. The data, i.e., T and V are divided in two groups: 1. the data for modeling and 2. the data for validating.
- (2) Establish procedures for modeling the first group of data and for explaining the second group of data. Calculate the models' error and identify the procedures reporting the lower mean error, i.e., the suitable proposals to describe the T and V patterns.

2. Materials and Methods

2.1. Simulation Settings

As previously stated, in a simulation, we have fast and slow vehicles. The fast vehicles are represented by the p_1 percentage and their speed tendency is sp_1 . The slow vehicles are represented by the p_2 percentage and their speed tendency is sp_2 . The speed tendency (or desired speed) is the speed that a driver aims to reach and tries to maintain, without exceeding it. Moreover, the fast drivers' desired speed is assumed to be the legal speed limit (or posted speed), and is selected in the range of 60 to 90 km/h. The slow drivers' desired speed is the half of their counterpart (fast drivers), and is selected in the range of 30 to 45 km/h. The desired speed values are selected in a range that will provide meaningful results for different traffic scenarios.

The simulation scenario is a two-lane one-direction avenue segment of $d = 500$ m length, with constant flow and no entry points, and (looking for general results) without considering specific road geometry or environmental issues. The input of a simulation are fast and slow speed tendency, sp_1 and sp_2 , respectively, and fast and slow vehicles' percentage, p_1 and p_2 , respectively. The output of a simulation are the fast vehicles' travel times. This outcome depends on the percentage of fast and slow vehicles and their speed tendencies.

For simulating we use the simulator tool presented in [2], which integrates the microsimulation model for accelerating (decelerating) in free driving and following another vehicle, as well as for overtaking. Thus, the fast vehicles' percentage and speed tendency can take a value from the sets $\{90\%, 80\%, \dots, 20\%\}$ and $\{60 \text{ km/h}, 65 \text{ km/h}, 70 \text{ km/h}, \dots, 90 \text{ km/h}\}$, respectively. p_2 can take a value from the set $\{10\%, 20\%, \dots, 80\%\}$, while sp_2 can take a value from the set $\{30 \text{ km/h}, 32.5 \text{ km/h}, 35 \text{ km/h}, \dots, 45 \text{ km/h}\}$. Recalling that $p_1 = 100\% - p_2$ and $sp_2 = sp_1/2$, a p_2 value fixes p_1 , and a sp_1 value fixes sp_2 . In a simulation, the fast vehicles' travel time to complete the 500 m distance is being measured, which is influenced by the slow vehicles, because these force the fast vehicles to perform overtaking maneuvers. We have eight simulations (the possible values of p_2) for each of the seven sp_1 cases, thus 56 simulations were performed. We use the output data of 40 simulations (hereafter, data for modeling) for modeling, in these simulations sp_1 is a value from

{60,65,75,85,90}. We use the output data of 16 simulations (hereafter, data for validating) for validating, in these simulations sp_1 is a value from {70,80}. The data for modeling and validating conform the total observed data. The simulation time of a single simulation is 600 s, thus the total simulation time was 33600 s, or 9.3333 h. For all simulations, we set the time lapse (f) between vehicles' arrival per lane to be $f = 6$ s, i.e., one vehicle arrives per lane each 6 s. Table 1 shows the parameters' values for setting a simulation. As the flow is constant, the time of day and day of week, which are variables related with demand, were out of the scope of this study. Instead, variables p_2 and sp_1 (and their counterparts, p_1 and sp_2 , respectively) shape the traffic outcome (travel times).

Table 1. Simulation settings.

Fast Vehicles' Desired Speed (km/h)	Slow Vehicles' Desired Speed (km/h)	Fast Vehicles' Percentage (%)	Slow Vehicles' Percentage (%)	Time Lapse between Vehicles per Lane (s)
A value of the set {60,65, ..., 85,90}	A value of the set {30,32.5, ..., 42.5,45}	A value of the set {90,80, ..., 30,20}	A value of the set {10,20, ..., 70,80}	6 s

When a vehicle is generated in a simulation, we need to establish if it will be a fast or a slow one. In any simulation, for each 10 vehicles generated (a group), it is guaranteed that the percentages of fast and slow vehicles of that group are equal to the percentages' values (p_1 and p_2 , respectively) of the simulation settings. This generation process seeks to avoid patterns between groups in the order by which the fast and slow vehicles are generated, but there is also randomness involved. For completeness, we repeated simulations for various selections of sp_1 and p_2 values, as the order of the generated vehicles will be different from one simulation to another and thus the outcome will be different too. We compare the T of simulations with same sp_1 and p_2 values and were not statistically different. The same applies for V .

2.2. Traffic Data

The travel time of the i -th vehicle (of those that count for p_1) is $t_i = t_i^{out} - t_i^{in}$, where t_i^{out} is the timestamp (in seconds, the time starts as the simulation does) when the i -th vehicle leaves the avenue, and t_i^{in} is the timestamp when the i -th vehicle enters the avenue. The expected travel time (t^{sp}) is calculated using Equation (1). As sp_1 is assumed to be the legal speed limit, it is also the maximum speed to travel along the distance d . Therefore, t^{sp} is the minimum time (without any delay) to traverse d .

$$t^{sp} = d/sp_1 \quad (1)$$

The mean extra travel time (T) is calculated with Equation (2).

$$T = \sum_{i=1}^N (t_i - t^{sp}) / N \quad (2)$$

where $i = 1 \dots N$ is the vehicle index, and N is the total number of fast vehicles during the simulation. Table 2 shows the T of the simulations with modeling purposes, so $T_{sp_1}^{p_2} = T_{60}^{10} = 0.232 \times 10^{-3}$ s is the mean extra travel time from a simulation with $p_2 = 10\%$ and $sp_1 = 60$ km/h.

Extra travel time variability is calculated with Equation (3), similar as in the study presented in [37].

$$V = \frac{1}{N} \sum_{i=1}^N |t_i^e - T| \quad (3)$$

In Equation (3), V is the extra travel time variability and $t_i^e = t_i - t^{sp}$ is the extra travel time of the i -th vehicle. The calculated V values in Table 3, where $V_{sp_1}^{p_2} = V_{90}^{80} = 1.105068$ s, correspond to a simulation with $p_2 = 80\%$ and $sp_1 = 90$ km/h.

Table 2. Mean extra travel time data.

p_2	T_{60}	T_{65}	T_{75}	T_{85}	T_{90}
10%	$T_{60}^{10} = 0.232 \times 10^{-3}$ s	$T_{65}^{10} = 0.011688$	$T_{75}^{10} = 0.066858$	$T_{85}^{10} = 0.09583$	$T_{90}^{10} = 0.052981$
20%	$T_{60}^{20} = 0.255986$	0.335886	0.321614	0.393612	0.315841
30%	$T_{60}^{30} = 0.915285$	0.813281	0.75368	0.823075	0.784827
40%	$T_{60}^{40} = 1.944888$	1.609535	1.718255	1.379915	1.400379
50%	$T_{60}^{50} = 3.237528$	2.881251	2.453064	2.20284	2.190038
60%	$T_{60}^{60} = 4.812069$	4.316362	3.70371	3.239808	3.135533
70%	$T_{60}^{70} = 6.774603$	6.005609	4.949776	4.394159	4.239621
80%	$T_{60}^{80} = 9.029137$	7.842978	6.649683	5.68031	5.467405

Table 3. Extra travel time variability data.

p_2	V_{60}	V_{65}	V_{75}	V_{85}	V_{90}
10%	$V_{60}^{10} = 5.28 \times 10^{-5}$ s	$V_{65}^{10} = 0.011465$	$V_{75}^{10} = 0.082488$	$V_{85}^{10} = 0.119821$	$V_{90}^{10} = 0.072548$
20%	$V_{60}^{20} = 0.375195$	0.452188	0.347738	0.409435	0.341801
30%	$V_{60}^{30} = 0.89158$	0.681472	0.605966	0.583584	0.530159
40%	$V_{60}^{40} = 1.194243$	0.888504	0.891808	0.768092	0.788808
50%	$V_{60}^{50} = 1.666407$	1.207142	1.279672	1.250472	1.477645
60%	$V_{60}^{60} = 1.350847$	1.152442	1.290058	1.167536	1.054867
70%	$V_{60}^{70} = 1.612525$	1.612141	1.413731	1.062381	1.236766
80%	$V_{60}^{80} = 1.31128$	1.257396	0.996451	1.23536	1.105068

2.3. Modeling T

2.3.1. Procedure 1

T values corresponding to $sp_1 = 60$ km/h and p_2 selections (second data column in Table 2 above) are stored in vector $A_{60} = [0.23 \times 10^{-3} \ 0.25 \dots 6.77 \ 9.02]$. The same procedure can be used to construct a vector for each sp_1 case. A vector content is accessed by position with index $j = 1 \dots 8$, for example $A_{65}(1) = 0.0116$. We construct vector B_{sp_1} with A_{sp_1} in such a way that, for $j \geq 2$, $B_{sp_1}(j-1) = A_{sp_1}(j) - A_{sp_1}(j-1)$, because the values of vectors B_{sp_1} might follow a linear pattern. Table 4 presents the values of vectors B_{sp_1} . In the first column, we have the content of vector B_{60} ; in the second, the content of B_{65} ; and so on.

The Pearson's linear correlation coefficient (r) between vector B_{sp_1} and vector $J = [1 \ 2 \dots 6 \ 7]$ (the vector containing the $j = 1 \dots 7$ index values) is expressed as $\text{corr}(B_{sp_1}, J)$. As $\text{corr}(B_{sp_1}, J) \geq 0.95$ for sp_1 values $\{60, 65, 75, 85, 90\}$, each B_{sp_1} vector is modeled with a linear equation (Equation (4)). The equations presented in this section, and in the following ones, were solved with the least-squares technique.

$$\check{B}_{sp_1}(j) = (a \cdot j) + b \quad (4)$$

With Equation (4) (with index j being the independent term), we calculate parameters a (slope) and b (y-intercept) for modeling vectors in Table 4, resulting in vectors \check{B}_{sp_1} . Table 5 presents parameters a and b to obtain each vector \check{B}_{sp_1} . In the first column, the parameters' values for obtaining $\check{B}_{sp_1=60}$ can be found; in the second, those for \check{B}_{65} ; and so on. Parameter

a values are in vector P_a , so $P_a = [0.32 \ 0.27 \ 0.22 \ 0.17 \ 0.16]$; while parameter b values are in vector P_b , so $P_b = [-0.01 \ 0.03 \ 0.04 \ 0.09 \ 0.13]$.

Table 4. Vectors B_{sp_1} values.

$B_{sp_1=60}$	$B_{sp_1=65}$	$B_{sp_1=75}$	$B_{sp_1=85}$	$B_{sp_1=90}$
$B_{60}(1) = 0.255754 \text{ s}$	$B_{65}(1) = 0.324197$	$B_{75}(1) = 0.254756$	$B_{85}(1) = 0.297783$	$B_{90}(1) = 0.26286$
$B_{60}(2) = 0.659299$	0.477396	0.432067	0.429463	0.468985
$B_{60}(3) = 1.029603$	0.796253	0.964575	0.55684	0.615552
$B_{60}(4) = 1.29264$	1.271716	0.734809	0.822926	0.789659
$B_{60}(5) = 1.574541$	1.435111	1.250645	1.036968	0.945494
$B_{60}(6) = 1.962534$	1.689247	1.246066	1.154351	1.104088
$B_{60}(7) = 2.254534$	1.837369	1.699908	1.286151	1.227784

Table 5. Vector \check{B}_{sp_1} parameters' values (procedure 1).

Parameter	$\check{B}_{sp_1=60}$	$\check{B}_{sp_1=65}$	$\check{B}_{sp_1=75}$	$\check{B}_{sp_1=85}$	$\check{B}_{sp_1=90}$
a	0.3267	0.2715	0.2231	0.1748	0.1605
b	−0.0169	0.0327	0.0476	0.0984	0.1313

Consider now parameter a values in P_a with position values $X_1 = [1 \ 2 \ 4 \ 6 \ 7]$, which are the positions corresponding to the sp_1 values $\{60, 65, 75, 85, 90\}$. Position 1 corresponds to a parameter for describing B_{60} , and position 2 for B_{65} , thus missing positions 3 and 5, which correspond with B_{70} and B_{80} , respectively. X_1 and P_a are negatively correlated ($r = -0.9849$), while X_1 and P_b are positively correlated ($r = 0.9772$). Then, by solving a linear equation relating X_1 and P_a , we calculate parameter \tilde{a} values for $X_2 = [3 \ 5]$, which are the positions corresponding to the sp_1 cases $\{70, 80\}$. The same path is taken for calculating parameter \tilde{b} values through a linear equation, now relating X_1 and P_b . The models and their statistics are presented in Table 6. Thus, with the models in Table 6 and $x = 3$, we obtain \tilde{a} and \tilde{b} parameters' values for estimating vector \hat{B}_{70} , and with $x = 5$, we obtain the parameters' values to estimate vector \hat{B}_{80} . Table 7 presents \tilde{a} and \tilde{b} parameters' values, used in $\hat{B}_{sp_1}(j) = (\tilde{a} \cdot j) + \tilde{b}$.

Table 6. Parameters' models and statistics (procedure 1).

Model	Root Mean Squared Error	R-Squared	Adjusted R-Squared	p-Value
$\tilde{a} = -0.0266 x + 0.3378$	0.0138	0.97	0.96	0.00223
$\tilde{b} = 0.0222 x - 0.0300$	0.0142	0.955	0.94	0.00412

Table 7. Vector \hat{B}_{sp_1} parameters' values (procedure 1).

Parameter	$\hat{B}_{sp_1=70}$	$\hat{B}_{sp_1=80}$
\tilde{a}	0.2579	0.2047
\tilde{b}	0.0364	0.0808

A vector \hat{B}_{sp_1} is transformed to \hat{A}_{sp_1} in such a way that $\hat{A}_{70}(1)$ and $\hat{A}_{80}(1)$ are inferred through linear regression using values $[A_{65}(1) \ A_{75}(1) \ A_{85}(1)]$; for $k \geq 2$, $\hat{A}_{sp_1}(k) = \hat{A}_{sp_1}(1) + \sum_{j=1}^{k-1} \hat{B}_{sp_1}(j)$. A vector \check{B}_{sp_1} is transformed to \check{A}_{sp_1} such that $\check{A}_{sp_1}(1) = A_{sp_1}(1)$; for $k \geq 2$, $\check{A}_{sp_1}(k) = \check{A}_{sp_1}(1) + \sum_{j=1}^{k-1} \check{B}_{sp_1}(j)$.

2.3.2. Procedure 2

Now, vectors A_{sp_1} for sp_1 values {60,65,75,85,90} are modeled with the exponential function presented in Equation (5), with p_2 (the slow vehicles' percentage value) being the independent term, c and d being the model's parameters, and index $k = 1 \dots 8$. The exponential function's parameters' values to obtain vectors \check{A}_{sp_1} are presented in Table 8.

$$\check{A}_{sp_1}(k) = c \cdot \exp(d \cdot p_2) \quad (5)$$

Table 8. Vectors \check{A}_{sp_1} parameters' values (procedure 2).

Parameter	$\check{A}_{sp_1=60}$	$\check{A}_{sp_1=65}$	$\check{A}_{sp_1=75}$	$\check{A}_{sp_1=85}$	$\check{A}_{sp_1=90}$
c	$c = 0.4167$	0.3817	0.3612	0.3440	0.3379
d	$d = 0.0389$	0.0384	0.0368	0.0356	0.0353

Parameter c values in vector $P_c = [0.4167 \dots 0.3379]$, and parameter d values in vector $P_d = [0.0389 \dots 0.0353]$. The correlation coefficient between X_1 and P_c is $r = -0.9567$, and that between X_1 and P_d is $r = -0.9943$. Thus, by means of a linear equation with independent values being X_1 and dependent values being P_c , we calculate parameter \tilde{c} at X_2 values. The same method is used for calculating parameter \tilde{d} at X_2 values with the derived linear model of X_1 versus P_d . Models and statistics for \tilde{c} and \tilde{d} are presented in Table 9. The parameters' values displayed in Table 10 are used in $\hat{A}_{sp_1}(k) = \tilde{c} \cdot \exp(\tilde{d} \cdot p_2)$.

Table 9. Parameters' models and statistics (procedure 2).

Model	Root Mean Squared Error	R-Squared	Adjusted R-Squared	p-Value
$\tilde{c} = -0.0120 x + 0.4163$	0.0107	0.915	0.887	0.0107
$\tilde{d} = -0.0006 x + 0.0396$	0.000199	0.989	0.985	0.000515

Table 10. Vectors \hat{A}_{sp_1} parameters' values (procedure 2).

Parameter	$\hat{A}_{sp_1=70}$	$\hat{A}_{sp_1=80}$
\tilde{c}	0.3803	0.3563
\tilde{d}	0.0376	0.0364

2.3.3. Procedure 3

Now, vectors A_{sp_1} for sp_1 cases {60,65,75,85,90} are modeled with a polynomial equation, with p_2 being the independent term; see Equation (6).

$$\check{A}_{sp_1}(k) = a_1 p_2^n + a_2 p_2^{n-1} + \dots + a_n p_2 + a_{n+1} \quad (6)$$

We choose $n = 2$ (three parameters) for the polynomial order because the mean error $\bar{E} = \text{mean}([E_{60} E_{65} E_{75} E_{85} E_{90}]) = 0.0356$ s is acceptable, where E_{sp_1} is the error of comparing A_{sp_1} and \check{A}_{sp_1} . Choosing $n = 3$ results in $\bar{E} = 0.0295$ s, which is not a significant improvement (a lower error). The parameters' values of $\check{A}_{sp_1}(k) = a_1 p_2^2 + a_2 p_2^1 + a_3$ are presented in Table 11. The a_1 parameter values in $P_{a_1} = [0.0016 \dots 0.0008]$, a_2 parameter values in $P_{a_2} = [-0.0159 \dots 0.0055]$, and a_3 parameter values in $P_{a_3} = [-0.0328 \dots -0.0991]$.

Table 11. Vectors \check{A}_{sp_1} parameters' values (procedure 3).

Parameter	$\check{A}_{sp_1=60}$	$\check{A}_{sp_1=65}$	$\check{A}_{sp_1=75}$	$\check{A}_{sp_1=85}$	$\check{A}_{sp_1=90}$
a_1	0.0016	0.0013	0.0010	0.0009	0.0008
a_2	−0.0159	−0.0127	−0.0029	−0.0010	0.0055
a_3	−0.0328	−0.0129	−0.0322	0.0278	−0.0991

The linear correlation coefficient between P_{a_1} and X_1 is $r = -0.9860$, that for P_{a_2} and X_1 is $r = 0.9788$, and that for P_{a_3} and X_1 is $r = -0.2513$. Considering r values, the \tilde{a}_1 and \tilde{a}_2 parameters were calculated using a linear equation, from P_{a_1} versus X_1 and P_{a_2} versus X_1 , respectively. The \tilde{a}_3 parameter was calculated using a polynomial equation of order $n = 4$, from P_{a_3} versus X_1 . The parameters' models and statistics are presented in Table 12, with these models we obtain \tilde{a}_1 , \tilde{a}_2 and \tilde{a}_3 for each value in X_2 . The parameters' values are used in $\hat{A}_{sp_1}(k) = \tilde{a}_1 p_2^2 + \tilde{a}_2 p_2 + \tilde{a}_3$ and presented in Table 13.

Table 12. Parameters' models and statistics (procedure 3).

Model	Root Mean Squared Error	R-Squared	p-Value
$\tilde{a}_1 = -0.0001 x + 0.0016$	6.58×10^{-5}	0.972	0.00199
$\tilde{a}_2 = 0.0033 x - 0.0189$	0.00208	0.958	0.0037
$\tilde{a}_3 = -0.0027 x^4 + 0.0395 x^3 - 0.1907 x^2 + 0.3565 x - 0.2353$	0	1	—

Table 13. Vectors \hat{A}_{sp_1} parameters' values (procedure 3).

Explained Vector	Parameter \tilde{a}_1	Parameter \tilde{a}_2	Parameter \tilde{a}_3
$\hat{A}_{sp_1=70}$	0.00129	−0.0087	−0.0370
$\hat{A}_{sp_1=80}$	0.0010	−0.0020	0.0087

2.4. Modeling V

2.4.1. Procedure 4

Mean extra travel time might explain extra travel time variability. The Pearson's linear correlation coefficient (r) between T values (in vector A_{sp_1} , corresponding to $p_2 = 10\%$ to 80%) and V values (in vector C_{sp_1}) is expressed as $\text{corr}(A_{sp_1}, C_{sp_1})$. For the different sp_1 cases, $\text{corr}(A_{60}, C_{60}) = 0.7054$, $\text{corr}(A_{65}, C_{65}) = 0.8334$, $\text{corr}(A_{75}, C_{75}) = 0.7361$, $\text{corr}(A_{85}, C_{85}) = 0.8268$, and $\text{corr}(A_{90}, C_{90}) = 0.7543$. There is a positive correlation between A_{sp_1} and C_{sp_1} for any sp_1 case, thus if T increases, so does V . Now, we use a polynomial equation to explain V with T , i.e., the independent values in A_{sp_1} and the dependent values in C_{sp_1} . We propose that the choice of the polynomial equation degree should satisfy two conditions: the mean error $\bar{E} = \text{mean}([E_{60} E_{65} E_{75} E_{85} E_{90}]) < 0.1$, where E_{sp_1} is the error between C_{sp_1} and \check{C}_{sp_1} , and the correlation coefficient $|r| > 0.60$ for each vector's parameter values and X_1 . A polynomial equation of order $n = 3$ satisfies both conditions. Then, $\check{C}_{sp_1}(k) = b_1 A_{sp_1}(k)^3 + b_2 A_{sp_1}(k)^2 + b_3 A_{sp_1}(k) + b_4$; the parameters' values are shown in Table 14. Vector $P_{b_1} = [0.0077 \dots 0.0168]$ contains the b_1 parameter values for sp_1 cases $\{60, 65, 75, 85, 90\}$, $P_{b_2} = [-0.1473 \dots -0.2285]$, $P_{b_3} = [0.8393 \dots 0.9467]$, and $P_{b_4} = [0.1177 \dots 0.0084]$.

Table 14. Vectors \check{C}_{sp_1} parameters' values (procedure 4).

Parameter	$\check{C}_{sp_1=60}$	\check{C}_{65}	\check{C}_{75}	\check{C}_{85}	\check{C}_{90}
b_1	0.0077	0.0031	0.0022	0.0221	0.0168
b_2	−0.1473	−0.0763	−0.0943	−0.2551	−0.2285
b_3	0.8393	0.5507	0.6649	0.9454	0.9467
b_4	0.1177	0.1706	0.0992	0.0200	0.0084

Thus, we obtain vectors \check{C}_{sp_1} with parameters in Table 14. For modeling $\tilde{b}_1, \tilde{b}_2, \tilde{b}_3$, and \tilde{b}_4 we use a polynomial equation of order $n = 3$. For \tilde{b}_1 , we have P_{b_1} (dependent values) and X_1 (independent values), and so on for \tilde{b}_2, \tilde{b}_3 , and \tilde{b}_4 considering P_{b_2}, P_{b_3} , and P_{b_4} , respectively. The parameters' models and statistics are presented in Table 15, where the models explain well (R-squared in the range $\sim 87\%$ to $\sim 99\%$) the dependent variable (a parameter). The parameters' values for estimating $\hat{C}_{sp_1}(k) = \tilde{b}_1 A_{sp_1}(k)^3 + \tilde{b}_2 A_{sp_1}(k)^2 + \tilde{b}_3 A_{sp_1}(k) + \tilde{b}_4$ are presented in Table 16.

Table 15. Parameters' models and statistics (procedure 4).

Model	Root Mean Squared Error	R-Squared	p-Value
$\tilde{b}_1 = -0.0006 x^3 + 0.0086 x^2 - 0.0305 x + 0.0317$	0.00624	0.873	0.445
$\tilde{b}_2 = 0.0062 x^3 - 0.0839 x^2 + 0.303 x - 0.3799$	0.0313	0.961	0.249
$\tilde{b}_3 = -0.0161 x^3 + 0.2199 x^2 - 0.8209 x + 1.452$	0.0192	0.997	0.0692
$\tilde{b}_4 = 0.0038 x^3 - 0.0511 x^2 + 0.1695 x - 0.0015$	0.0128	0.991	0.119

Table 16. Vectors \hat{C}_{sp_1} parameters' values (procedure 4).

Vector	\tilde{b}_1	\tilde{b}_2	\tilde{b}_3	\tilde{b}_4
$\hat{C}_{sp_1=70}$	0.0078	−0.1372	0.7466	0.1074
\hat{C}_{80}	0.0129	−0.1834	0.8322	0.0590

2.4.2. Procedure 5

The linear correlation between $p = [10\ 20 \dots 70\ 80]$ (p_2 values) and C_{sp_1} (V values) for sp_1 cases $\{60, 65, 75, 85, 90\}$ is always positive and in the range of ~ 0.85 to ~ 0.93 . As the percentage of slow vehicles increases, extra travel time variability increases. Now, with a polynomial equation, the dependent variable V is explained by the independent variable p_2 . For the polynomial degree (starting with $n = 1$), we seek to meet two conditions (the same as in procedure 4): (1) $\bar{E} < 0.1$ and (2) $|r| > 0.60$ for each P_b vector. $\bar{E} = \text{mean}([E_{60}\ E_{65}\ E_{75}\ E_{85}\ E_{90}])$, where E_{sp_1} is the error between C_{sp_1} and \check{C}_{sp_1} , and $r = \text{corr}(P_b, X_1)$ is the linear correlation coefficient between P_b (a vector containing the b parameter values corresponding with the sp_1 cases) and X_1 . With $n = 5$, both conditions are met. The parameters' values for modeling $\check{C}_{sp_1}(k) = b_1 p_2^5 + b_2 p_2^4 + b_3 p_2^3 + b_4 p_2^2 + b_5 p_2 + b_6$ are presented in Table 17. The b_1 parameter values are in vector P_{b_1} , the b_2 parameter values are in vector P_{b_2} , and so on.

Each vector P_b was modeled with a linear equation, with X_1 as the independent values and P_b as the dependent values. The models and statistical results are shown in Table 18.

With the models in Table 18, we calculate each parameter for X_2 values (corresponding to sp_1 cases $\{70, 80\}$). The parameters' values for describing $\hat{C}_{sp_1}(k) = \tilde{b}_1 p_2^5 + \tilde{b}_2 p_2^4 + \tilde{b}_3 p_2^3 + \tilde{b}_4 p_2^2 + \tilde{b}_5 p_2 + \tilde{b}_6$ are presented in Table 19.

Table 17. Vectors \check{C}_{sp_1} parameters' values (procedure 5).

Vector	b_1	b_2	b_3	b_4	b_5	b_6
$\check{C}_{sp_1=60}$	-1.4070×10^{-8}	3.3891×10^{-6}	-0.3069×10^{-3}	0.0122	-0.1633	0.6934
\check{C}_{65}	-1.6574×10^{-8}	3.2941×10^{-6}	-0.2344×10^{-3}	0.0069	-0.0506	0.0313
\check{C}_{75}	-2.1557×10^{-9}	3.4381×10^{-7}	-2.7155×10^{-5}	0.0012	0.0028	-0.0381
\check{C}_{85}	3.1903×10^{-8}	-6.8689×10^{-6}	0.5373×10^{-3}	-0.0188	0.3114	-1.5865
\check{C}_{90}	1.8897×10^{-8}	-3.9332×10^{-6}	0.2878×10^{-3}	-0.0090	0.1463	-0.7256

Table 18. Models and statistics (procedure 5).

Model	Root Mean Squared Error	R-Squared	p-Value
$\tilde{b}_1 = 7.5331 \times 10^{-9} x - 2.6532 \times 10^{-8}$	1.02×10^{-8}	0.825	0.0328
$\tilde{b}_2 = -1.6267 \times 10^{-6} x + 5.7517 \times 10^{-6}$	2.12×10^{-6}	0.836	0.0296
$\tilde{b}_3 = 0.000128 x - 0.00046068$	0.000166	0.838	0.0292
$\tilde{b}_4 = -0.0044404 x + 0.016265$	0.0061	0.821	0.0341
$\tilde{b}_5 = 0.063598 x - 0.20505$	0.101	0.776	0.0485
$\tilde{b}_6 = -0.2882 x + 0.82771$	0.529	0.72	0.627

Table 19. Vectors \hat{C}_{sp_1} parameters' values (procedure 5).

Vector	\tilde{b}_1	\tilde{b}_2	\tilde{b}_3	\tilde{b}_4	\tilde{b}_5	\tilde{b}_6
$\hat{C}_{sp_1=70}$	-3.9331×10^{-9}	8.7164×10^{-7}	-7.6672×10^{-5}	0.0029	-0.0142	-0.0368
$\hat{C}_{sp_1=80}$	1.1133×10^{-8}	-2.3817×10^{-6}	0.1793×10^{-3}	-0.0059	0.1129	-0.6132

2.4.3. Procedure 6

The linear correlation coefficient between $P_1 = [10 \ 20 \ 30 \ 40]$ (p_2 values from 10% to 40%) and $C_{sp_1}(1 : 4)$ is $\text{corr}(P_1, C_{sp_1}(1 : 4)) \geq 0.98$ for all sp_1 cases $\{60, 65, 75, 85, 90\}$. Between $P_2 = [50 \ 60 \ 70 \ 80]$ (p_2 values from 50% to 80%) and $C_{sp_1}(5 : 8)$ are the following: $\text{corr}(P_2, C_{60}(5 : 8)) = -0.5759$, $\text{corr}(P_2, C_{65}(5 : 8)) = 0.3794$, $\text{corr}(P_2, C_{75}(5 : 8)) = -0.5309$, $\text{corr}(P_2, C_{85}(5 : 8)) = -0.2267$, and $\text{corr}(P_2, C_{90}(5 : 8)) = -0.6393$. In $C_{sp_1}(1 : 4)$, the first four values, and in $C_{sp_1}(5 : 8)$, the last four values of C_{sp_1} . There is a strong positive correlation between P_1 and $C_{sp_1}(1 : 4)$ for all sp_1 cases. The correlations between P_2 and $C_{sp_1}(5 : 8)$ cases are not that strong. Thus, we modeled (independent variable p_2 and dependent variable V) a vector C_{sp_1} in two parts: the first four points with a linear equation and the last four points with a polynomial equation. When modeling vectors $C_{sp_1}(1 : 4)$, we obtained parameter b_1 (in vector P_{b_1}) and b_2 (in vector P_{b_2}) values. The r between X_1 and P_{b_1} is -0.8604 , and that between X_1 and P_{b_2} is 0.8160 . $\bar{E} = 0.0141$ s, with E_{sp_1} expressing the error between $C_{sp_1}(1 : 4)$ and $\check{C}_{sp_1}(1 : 4)$. By modeling $C_{sp_1}(5 : 8)$, we obtained the c_1 , c_2 , and c_3 parameter's values (in vectors P_{c_1} , P_{c_2} , and P_{c_3} , respectively). We selected for modeling $C_{sp_1}(5 : 8)$ a polynomial of degree $n = 2$, as $\bar{E} = 0.0434 < 0.1$, and neither $n = 2$ nor $n = 3$ satisfy $|r| < 0.60$ for all correlations. Nevertheless, with $n = 2$, $\text{corr}(P_{c_1}, X_1) = 0.58$, $\text{corr}(P_{c_2}, X_1) = -0.59$ and $\text{corr}(P_{c_3}, X_1) = 0.57$ are good approximations. Henceforth, using parameters b_1 and b_2 , we modeled a vector $\check{C}_{sp_1}(k_1) = b_1 p_2 + b_2$, with $k_1 = 1 \dots 4$ and $p_2 = 10 \dots 40$ (see Table 20). With parameters c_1 , c_2 , and c_3 , we modeled a vector $\check{C}_{sp_1}(k_2) = c_1 p_2^2 + c_2 p_2 + c_3$, with $k_2 = 5 \dots 8$ and $p_2 = 50 \dots 80$ (see Table 21). Vector $P_{b_1} = [0.0409 \dots 0.0233]$ contains b_1 parameter values, and vector $P_{b_2} = [-0.4094 \dots -0.1509]$ contains b_2 parameter values. Vectors $P_{c_1} = [3.5789 \times 10^{-5} \dots 0.7276 \times 10^{-3}]$, $P_{c_2} = [-0.0126 \dots -0.1039]$, and $P_{c_3} = [2.1544 \dots 4.8104]$.

Table 20. Vectors $\check{C}_{sp_1}(1:4)$ parameters' values (procedure 6).

Parameter	$\check{C}_{60}(1:4)$	$\check{C}_{65}(1:4)$	$\check{C}_{75}(1:4)$	$\check{C}_{85}(1:4)$	$\check{C}_{90}(1:4)$
b_1	0.0409	0.0286	0.0268	0.0211	0.0233
b_2	−0.4094	−0.2066	−0.1895	−0.0595	−0.1509

Table 21. Vectors $\check{C}_{sp_1}(5:8)$ parameters' values (procedure 6).

Parameter	$\check{C}_{sp_1=60}(5:8)$	$\check{C}_{65}(5:8)$	$\check{C}_{75}(5:8)$	$\check{C}_{85}(5:8)$	$\check{C}_{90}(5:8)$
c_1	3.5789×10^{-5}	-0.7501×10^{-3}	−0.0010	0.6397×10^{-3}	0.7276×10^{-3}
c_2	−0.0126	0.1036	0.1317	−0.0846	−0.1039
c_3	2.1544	−2.1649	−2.6667	3.8998	4.8104

The derived linear models of X_1 vs. P_{b_1} and X_1 vs. P_{b_2} are presented in Table 22. The parameters' values (obtained with models in Table 22 at X_2 values) used in $\hat{C}_{sp_1}(k_1) = \tilde{b}_1 p_2 + \tilde{b}_2$ for sp_1 cases {70, 80} are displayed in Table 23.

Table 22. Models (for parameters \tilde{b}_1 and \tilde{b}_2) and statistics (procedure 6).

Model	Root Mean Squared Error	R-Squared	p-Value
$\tilde{b}_1 = -0.0026032 x + 0.038616$	0.00454	0.74	0.0613
$\tilde{b}_2 = 0.041151 x - 0.36784$	0.0858	0.666	0.0921

Table 23. Vectors $\hat{C}_{sp_1}(1:4)$ parameters' values (procedure 6).

Parameter	$\hat{C}_{70}(1:4)$	$\hat{C}_{80}(1:4)$
\tilde{b}_1	0.0308	0.0256
\tilde{b}_2	−0.2443	−0.1620

The parameter values in P_{c_1} , P_{c_2} , and P_{c_3} were modeled with a polynomial equation of order $n = 4$ (for modeling five points). The models and statistics are shown in Table 24. The calculated parameters' values (with models in Table 24 at X_2 values) used in $\hat{C}_{sp_1}(k_2) = \tilde{c}_1 p_2^2 + \tilde{c}_2 p_2 + \tilde{c}_3$ for sp_1 cases {70, 80} are shown in Table 25.

Table 24. Models (for parameters \tilde{c}_1 , \tilde{c}_2 , and \tilde{c}_3) and statistics (procedure 6).

Model	Root Mean Squared Error	R-Squared	p-Value
$\tilde{c}_1 = -1.8458 \times 10^{-5} x^4 + 0.00024889 x^3 - 0.00088743 x^2 + 0.00041101 x + 0.00028177$	0	1	—
$\tilde{c}_2 = 0.0018896 x^4 - 0.02386 x^3 + 0.066804 x^2 + 0.054576 x - 0.1121$	0	1	—
$\tilde{c}_3 = -0.04006 x^4 + 0.42626 x^3 - 0.22552 x^2 - 6.0257 x + 8.0195$	0	1	—

Table 25. Vectors $\hat{C}_{sp_1}(5:8)$ parameters' values (procedure 6).

Vector	\tilde{c}_1	\tilde{c}_2	\tilde{c}_3
$\hat{C}_{70}(5:8)$	−0.0012	0.1616	−3.8233
$\hat{C}_{80}(5:8)$	-0.2735×10^{-3}	0.0293	0.4973

3. Results

3.1. Procedure 1 Results

With Equation (7), we establish the error between vectors A_{sp_1} and \hat{A}_{sp_1} , or between vectors A_{sp_1} and \check{A}_{sp_1} , where $q = 8$ is the number of elements in A_{sp_1} . The error between vectors A_{sp_1} and \hat{A}_{sp_1} is expressed as $E_{sp_1}(A_{sp_1}, \hat{A}_{sp_1})$, and that between vectors A_{sp_1} and \check{A}_{sp_1} as $E_{sp_1}(A_{sp_1}, \check{A}_{sp_1})$. The errors between A_{sp_1} and \check{A}_{sp_1} (a vector directly modeled with the data for modeling) for sp_1 values $\{60, 65, 75, 85, 90\}$ are as follows: $E_{60}(A_{60}, \check{A}_{60}) = 0.0222$ s, $E_{65}(A_{65}, \check{A}_{65}) = 0.0519$ s, $E_{75}(A_{75}, \check{A}_{75}) = 0.0550$ s, $E_{85}(A_{85}, \check{A}_{85}) = 0.0238$ s, and $E_{90}(A_{90}, \check{A}_{90}) = 0.0128$ s. The errors between A_{sp_1} and \hat{A}_{sp_1} (a vector indirectly modeled with the data for modeling, without the data for validating) for sp_1 values $\{70, 80\}$ are as follows: $E_{70}(A_{70}, \hat{A}_{70}) = 0.1817$ s and $E_{80}(A_{80}, \hat{A}_{80}) = 0.2505$ s.

$$E_{sp_1} = \frac{\sum_{k=1}^{k=q} |A_{sp_1}(k) - \hat{A}_{sp_1}(k)|}{q} \quad (7)$$

The mean error of the A_{sp_1} vs. \check{A}_{sp_1} cases is $\bar{E} = \text{mean}([E_{60} \ E_{65} \ E_{75} \ E_{85} \ E_{90}]) = 0.0332$ s, a lesser value than the mean error between the A_{sp_1} vs. \hat{A}_{sp_1} cases, which is $\bar{E} = \text{mean}([E_{70} \ E_{80}]) = 0.2162$ s. This is an expected result as vectors \check{A}_{sp_1} were modeled directly with the data for modeling, i.e., with A_{sp_1} for sp_1 values $\{60, 65, 75, 85, 90\}$, while vectors \hat{A}_{sp_1} were indirectly modeled with the data for modeling, but without the data for validating, i.e., without A_{sp_1} for sp_1 values $\{70, 80\}$. Figure 1 shows the graphs of the compared vectors in this section.

3.2. Procedure 2 Results

Vectors \hat{A}_{sp_1} for sp_1 values $\{70, 80\}$ were obtained with the parameters' values in Table 10 and Equation (5), and vectors \check{A}_{sp_1} for sp_1 values $\{60, 65, 75, 85, 90\}$ were obtained with the parameters' values in Table 8 and Equation (5). The errors between the A_{sp_1} and \check{A}_{sp_1} cases are as follows: $E_{60}(A_{60}, \check{A}_{60}) = 0.4151$ s, $E_{65}(A_{65}, \check{A}_{65}) = 0.3944$ s, $E_{75}(A_{75}, \check{A}_{75}) = 0.2957$ s, $E_{85}(A_{85}, \check{A}_{85}) = 0.2390$ s, and $E_{90}(A_{90}, \check{A}_{90}) = 0.2497$ s. The errors between the A_{sp_1} and \hat{A}_{sp_1} cases are as follows: $E_{70}(A_{70}, \hat{A}_{70}) = 0.3582$ s and $E_{80}(A_{80}, \hat{A}_{80}) = 0.4095$ s. The error of the directly modeled vectors \check{A}_{sp_1} is comparable to the error of the indirectly modeled vectors \hat{A}_{sp_1} . Figure 2 shows the graphs of the compared vectors in this section.

3.3. Procedure 3 Results

The errors between vectors \check{A}_{sp_1} and A_{sp_1} (directly estimated T vs. data for modeling) cases are as follows: $E_{60}(A_{60}, \check{A}_{60}) = 0.0226$ s, $E_{65}(A_{65}, \check{A}_{65}) = 0.0552$ s, $E_{75}(A_{75}, \check{A}_{75}) = 0.0617$ s, $E_{85}(A_{85}, \check{A}_{85}) = 0.0264$ s, and $E_{90}(A_{90}, \check{A}_{90}) = 0.0116$ s. The errors between vectors \hat{A}_{sp_1} and A_{sp_1} (indirectly estimated T vs. data for validating) are as follows: $E_{70}(A_{70}, \hat{A}_{70}) = 0.1892$ s and $E_{80}(A_{80}, \hat{A}_{80}) = 0.2371$ s. Figure 3 shows the graphs of the compared vectors in this section.

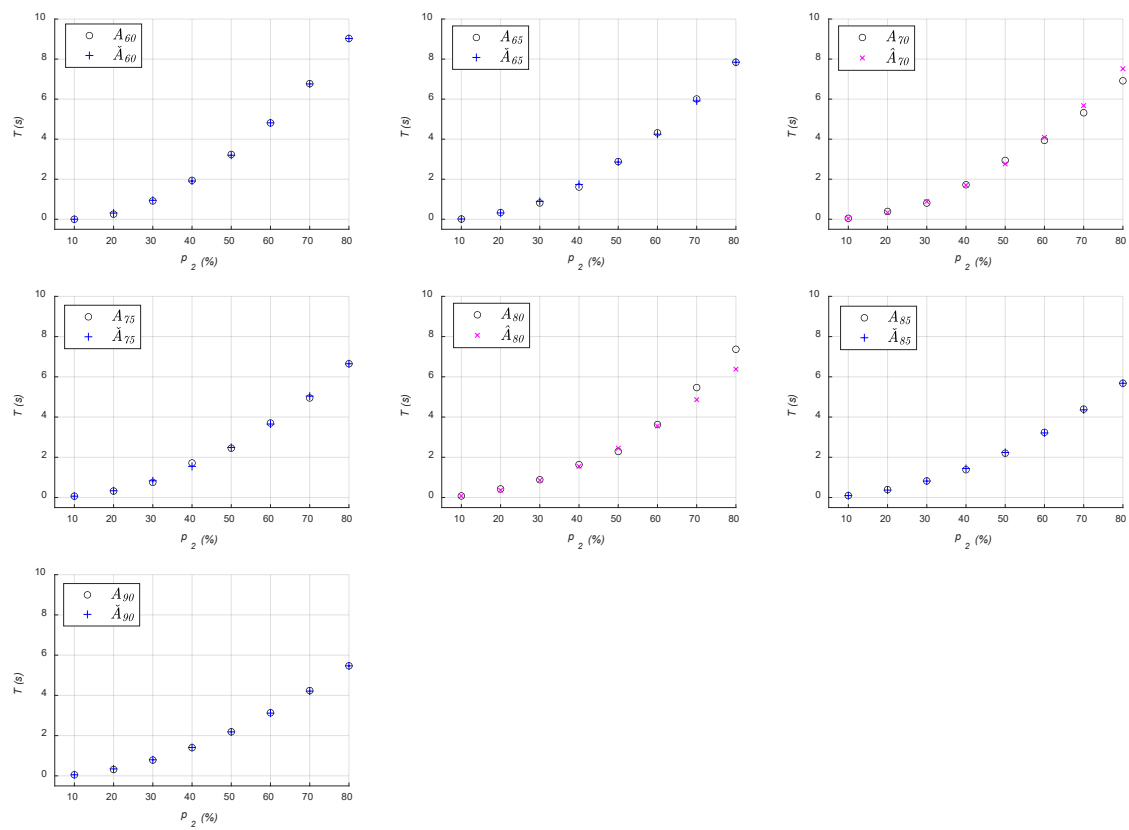


Figure 1. p_2 vs. T (procedure 1).

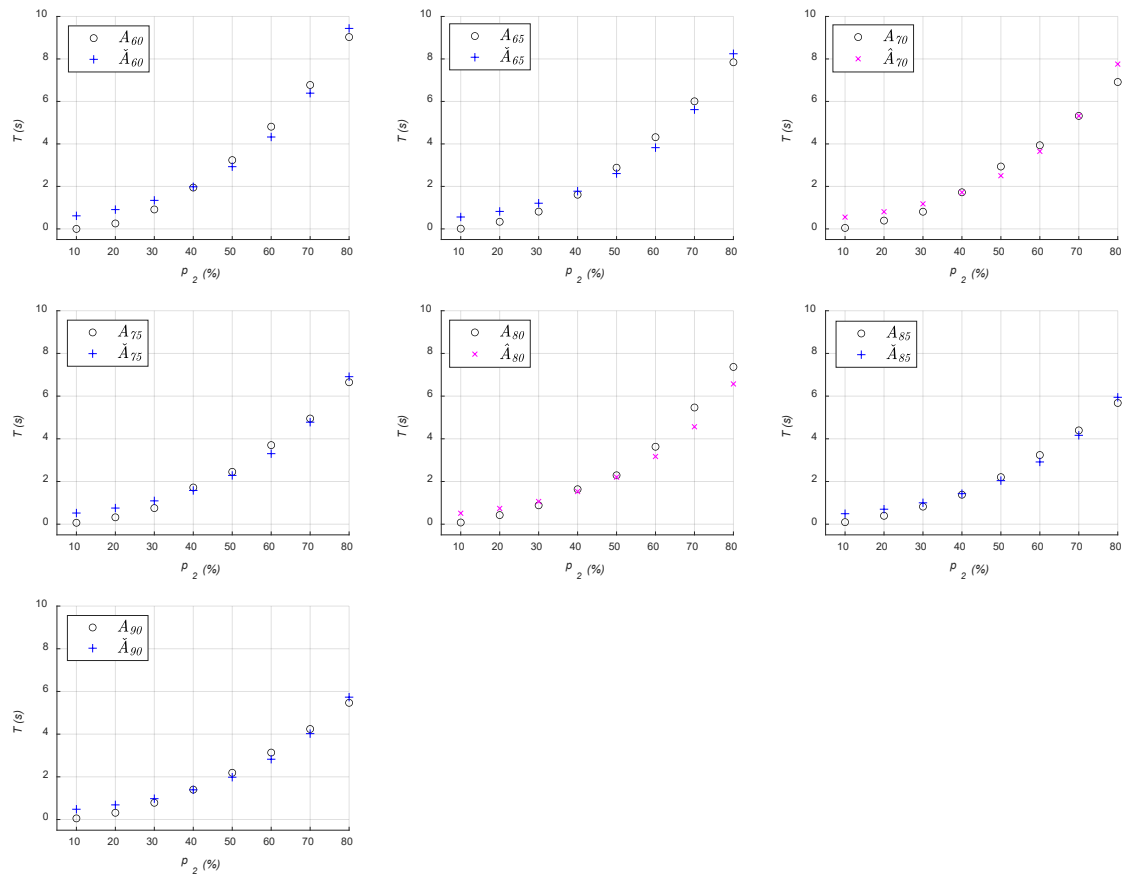


Figure 2. p_2 vs. T (procedure 2).

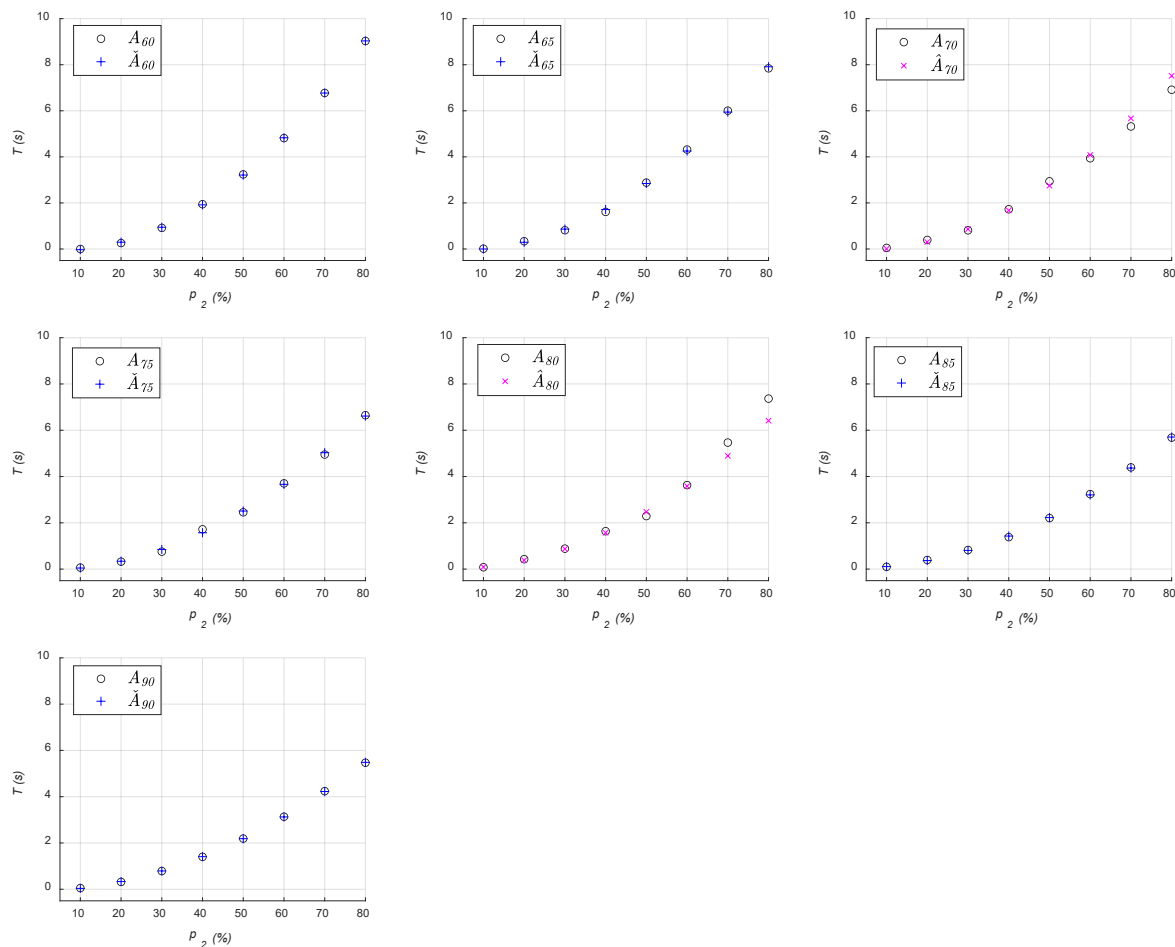


Figure 3. p_2 vs. T (procedure 3).

3.4. Procedure 4 Results

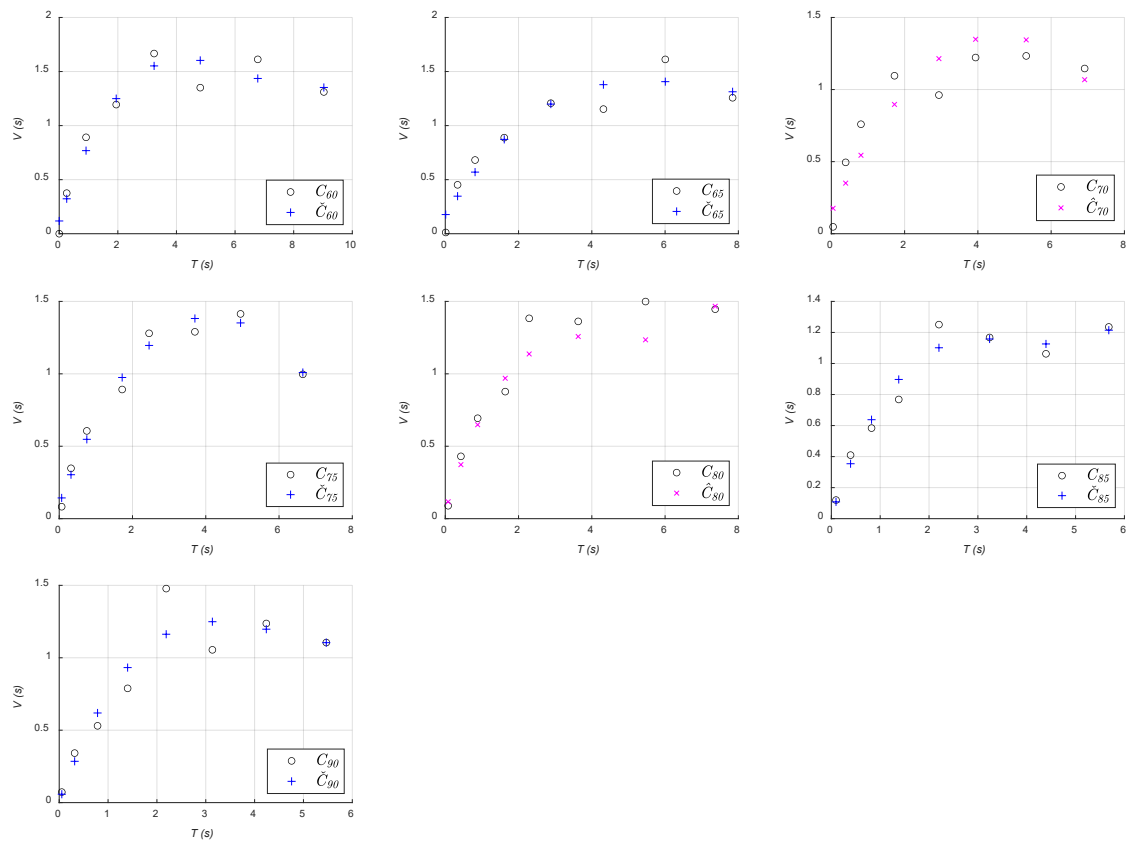
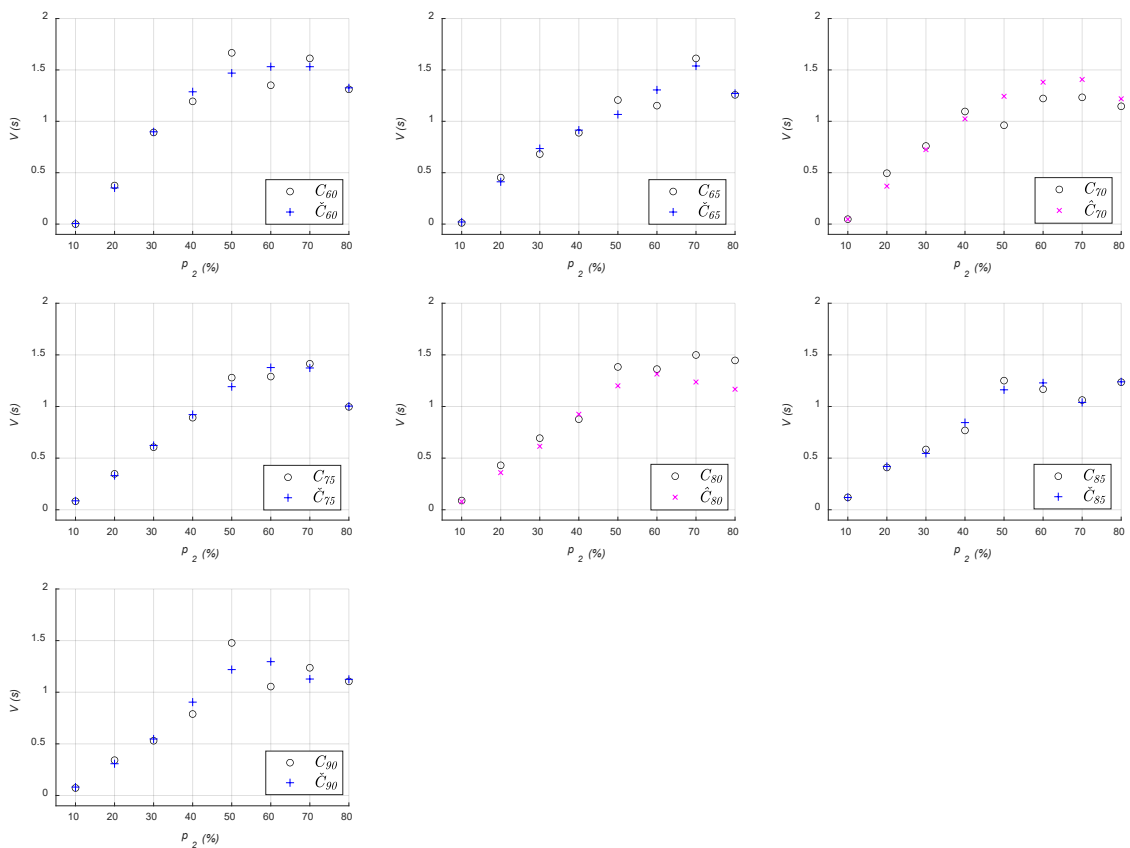
The errors between C_{sp_1} and \check{C}_{sp_1} for sp_1 values $\{60, 65, 75, 85, 90\}$ are: $E_{60}(A_{60}, \check{A}_{60}) = 0.1165$ s, $E_{65}(A_{65}, \check{A}_{65}) = 0.1117$ s, $E_{75}(A_{75}, \check{A}_{75}) = 0.0620$ s, $E_{85}(A_{85}, \check{A}_{85}) = 0.0616$ s, and $E_{90}(A_{90}, \check{A}_{90}) = 0.1065$ s. The errors between C_{sp_1} and \hat{C}_{sp_1} for sp_1 values $\{70, 80\}$ are: $E_{70}(A_{70}, \hat{A}_{70}) = 0.1569$ s and $E_{80}(A_{80}, \hat{A}_{80}) = 0.1070$ s. Figure 4 shows the graphs of the compared vectors in this section.

3.5. Procedure 5 Results

With the parameters' values from Table 17, we modeled vectors \check{C}_{sp_1} , and with the parameters values from Table 19, we estimated vectors \hat{C}_{sp_1} . The errors between the C_{sp_1} and \check{C}_{sp_1} cases are: $E_{60}(A_{60}, \check{A}_{60}) = 0.0753$ s, $E_{65}(A_{65}, \check{A}_{65}) = 0.0637$ s, $E_{75}(A_{75}, \check{A}_{75}) = 0.0362$ s, $E_{85}(A_{85}, \check{A}_{85}) = 0.0376$ s, and $E_{90}(A_{90}, \check{A}_{90}) = 0.1004$ s. The errors between the C_{sp_1} and \hat{C}_{sp_1} cases are: $E_{70}(A_{70}, \hat{A}_{70}) = 0.1150$ s and $E_{80}(A_{80}, \hat{A}_{80}) = 0.1223$ s. Figure 5 shows the graphs of the compared vectors in this section.

3.6. Procedure 6 Results

With parameters \tilde{b}_1 and \tilde{b}_2 (for a linear equation), we construct vectors $\hat{C}_{sp_1}(1 : 4)$. With parameters \tilde{c}_1 , \tilde{c}_2 , and \tilde{c}_3 (for an order 2 polynomial equation), we construct vectors $\hat{C}_{sp_1}(5 : 8)$. The errors between C_{sp_1} and \check{C}_{sp_1} for sp_1 cases $\{60, 65, 75, 85, 90\}$ are: $E_{60}(A_{60}, \check{A}_{60}) = 0.0748$ s, $E_{65}(A_{65}, \check{A}_{65}) = 0.0956$ s, $E_{75}(A_{75}, \check{A}_{75}) = 0.0352$ s, $E_{85}(A_{85}, \check{A}_{85}) = 0.0281$ s, and $E_{90}(A_{90}, \check{A}_{90}) = 0.0534$ s. The errors between C_{sp_1} and \hat{C}_{sp_1} for sp_1 cases $\{70, 80\}$ are: $E_{70}(A_{70}, \hat{A}_{70}) = 0.1051$ s and $E_{80}(A_{80}, \hat{A}_{80}) = 0.1285$ s. Figure 6 shows the graphs of the compared vectors in this section.

Figure 4. T vs. V (procedure 4).Figure 5. p_2 vs. V (procedure 5).

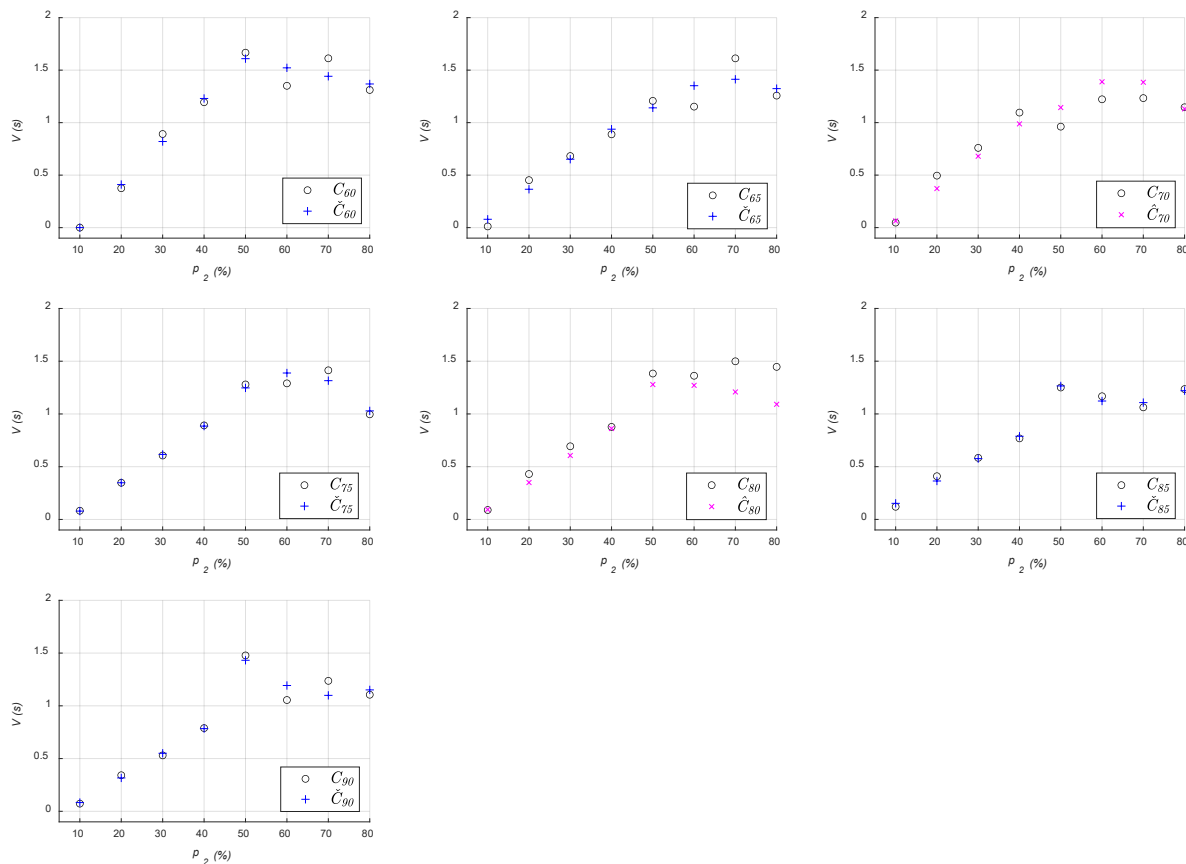


Figure 6. p_2 vs. V (procedure 6).

4. Discussion

4.1. Discussion for Explaining T

Table 26 presents the error (obtained in procedure 1, 2, and 3) between a vector with data for modeling (A_{sp1}) and the directly modeled vector (\check{A}_{sp1}). It also shows the mean of the errors $E_{sp1}(A_{sp1}, \check{A}_{sp1})$ for sp_1 cases $\{60, 65, 75, 85, 90\}$, i.e., $\bar{E} = \text{mean}([E_{60} \ E_{65} \ E_{75} \ E_{85} \ E_{90}])$. The lower mean error is presented by procedure 1, followed closely by procedure 3.

Table 26. Error between A_{sp1} and \check{A}_{sp1} (procedures 1, 2, and 3).

Procedure	$E_{60}(A_{60}, \check{A}_{60})$	$E_{65}(A_{65}, \check{A}_{65})$	$E_{75}(A_{75}, \check{A}_{75})$	$E_{85}(A_{85}, \check{A}_{85})$	$E_{90}(A_{90}, \check{A}_{90})$	\bar{E}
Procedure 1	0.0222 s	0.0519	0.0550	0.0238	0.0128	0.0332
Procedure 2	0.4151	0.3944	0.2957	0.2390	0.2497	0.3188
Procedure 3	0.0226	0.0552	0.0617	0.0264	0.0116	0.0355

Similarly, Table 27 presents the error between a vector with data for validating (A_{sp1}) and the indirectly modeled vector (\hat{A}_{sp1}). It also shows the mean of the errors $E_{sp1}(A_{sp1}, \hat{A}_{sp1})$ for sp_1 cases $\{70, 80\}$. The lower \bar{E} is presented by procedure 3, followed closely by procedure 1. Thus, the techniques presented in procedures 3 and 1 are the most suitable for modeling and explaining T .

We notice that, for procedures 1, 2, and 3, $E_{80} > E_{70}$, meaning that \hat{A}_{70} is easier to explain than \hat{A}_{80} . Moreover, for procedures 1 and 3, E_{65} and E_{75} are higher than E_{60} , E_{85} , and E_{90} . It follows that \hat{A}_{60} , \hat{A}_{85} , and \hat{A}_{90} are easier to model than \hat{A}_{65} and \hat{A}_{75} . In procedures 1 and 3, E_{90} presents the lowest error and E_{75} presents the highest, thus \hat{A}_{90} is the most easily modeled vector and \hat{A}_{75} is the hardest to model.

Table 27. Error between A_{sp_1} and \hat{A}_{sp_1} (procedures 1, 2, and 3).

Procedure #	$E_{70}(A_{70}, \hat{A}_{70})$	$E_{80}(A_{80}, \hat{A}_{80})$	$\bar{E} = \text{mean}([E_{70} E_{80}])$
Procedure 1	0.1817 s	0.2505	0.2162
Procedure 2	0.3582	0.4095	0.3839
Procedure 3	0.1892	0.2371	0.2132

In Figure 3, we observe that, for the sp_1 {70, 80} cases, the last two points of vectors \hat{A}_{sp_1} are clearly distant from the corresponding points of vectors A_{sp_1} (in contrast with the other six points). The last two points are the T when the percentage of slow vehicles is 70% and 80%. Hereafter, $\bar{E}^{x,y}$ is the mean error of the x {1, 2, ..., 5, 6} procedure and the y {1, 2} comparison, where $y = 1$ indicates a comparison between the directly modeled and observed data (Table 26 or Table 28), and $y = 2$ indicates a comparison between the not directly modeled and observed data (Table 27 or Table 29). Then, $\bar{E}^{3,2} = \text{mean}([E_{70}(A_{70}, \hat{A}_{70}) E_{80}(A_{80}, \hat{A}_{80})]) = 0.2132$ s is the mean error of procedure 3 and sp_1 {70, 80} cases.

Table 28. Error between C_{sp_1} and \check{C}_{sp_1} (procedures 4, 5, and 6).

Procedure #	$E_{60}(C_{60}, \check{C}_{60})$	$E_{65}(C_{65}, \check{C}_{65})$	$E_{75}(C_{75}, \check{C}_{75})$	$E_{85}(C_{85}, \check{C}_{85})$	$E_{90}(C_{90}, \check{C}_{90})$	\bar{E}
Procedure 4	0.1165 s	0.1117	0.0620	0.0616	0.1065	0.0917
Procedure 5	0.0753	0.0637	0.0362	0.0376	0.1004	0.0626
Procedure 6	0.0748	0.0956	0.0352	0.0281	0.0534	0.0574

Table 29. Error between C_{sp_1} and \hat{C}_{sp_1} (procedures 4, 5, and 6).

Procedure #	$E_{70}(C_{70}, \hat{C}_{70})$	$E_{80}(C_{80}, \hat{C}_{80})$	$\bar{E} = \text{mean}([E_{70} E_{80}])$
Procedure 4	0.1569 s	0.1070	0.1320
Procedure 5	0.1150	0.1223	0.1187
Procedure 6	0.1051	0.1285	0.1168

With procedure 1, the mean error between the directly modeled and observed data, i.e., $\bar{E}^{1,1} = 0.0332$ s, is lesser than the mean error between the not directly modeled and observed data, i.e., $\bar{E}^{1,2} = 0.2162$ s. This holds for the three procedures. Figure 1 shows that, for A_{sp_1} vs. \hat{A}_{sp_1} , the first six points of \hat{A}_{70} and \hat{A}_{80} are visible close to the corresponding points of A_{70} and A_{80} , respectively. The last two points of \hat{A}_{70} are above those of A_{70} , and the last two points of \hat{A}_{80} are below those of A_{80} .

In procedure 2, $E_{sp_1}(A_{sp_1}, \check{A}_{sp_1})$ varies between 0.2390 and 0.4151 s, and $\bar{E}^{2,1} = 0.3188$ s is not distant from $\bar{E}^{2,2} = \text{mean}([E_{70} E_{80}]) = 0.3839$ s, so the error of the directly modeled data $E_{sp_1}(A_{sp_1}, \check{A}_{sp_1})$ is similar to the error of the not directly modeled data $E_{sp_1}(A_{sp_1}, \hat{A}_{sp_1})$. Figure 2 shows that, for the directly modeled data (\check{A}_{sp_1}), the first three points are above the observed data (A_{sp_1}), point four is close (from above or below), points five to seven are below, and point eight is above. Comparing the indirectly modeled with the observed data, we notice that points 1, 2, and 3 of \hat{A}_{sp_1} are slightly above the corresponding points of A_{sp_1} (for sp_1 cases {70, 80}). For \hat{A}_{70} , the estimated points 4 and 7 are visibly accurate, the estimated points 5 and 6 are below the observed value, and the estimated point 8 is above the observed value. For \hat{A}_{80} , the estimated points 4 and 5 are visibly accurate, and the estimated points 6, 7, and 8 are below the observed value.

With these results, we found procedures 1 and 3 to be suitable to model the data for modeling and to explain the data for validating.

4.2. Discussion for Explaining V

Table 28 presents the error between the directly modeled data and data for modeling, with $\bar{E} = \text{mean}([E_{60} E_{65} E_{75} E_{85} E_{90}])$. Table 29 presents the error between the indirectly modeled data and data for validating, with $\bar{E} = \text{mean}([E_{70} E_{80}])$.

For modeling V , procedure 6 is the best option. Here, we have that $\bar{E}^{6,1} < \bar{E}^{5,1} < \bar{E}^{4,1}$ and that $\bar{E}^{6,2} < \bar{E}^{5,2} < \bar{E}^{4,2}$. Figure 6 shows that, in vectors \check{C}_{sp_1} for the sp_1 {60,65,75,90} cases, points 6 and 7 are the least accurate (i.e., dissimilar with the observed), with \check{C}_{85} being the most accurate ($E_{85} = 0.0281$ s) and \check{C}_{65} being the least accurate ($E_{65} = 0.0956$ s). In vector \hat{C}_{80} , points 7 and 8 are the least accurate; therefore, when $sp_1 = 80$ km/h and for $p_2 = 70\%$ and $p_2 = 80\%$, it was difficult to explain V .

In Figure 5, and regarding the directly modeled data, points 5 and 6 of vectors \check{C}_{sp_1} for the sp_1 {60,65,90} cases are visibly inaccurate, and points 4 to 7 of vector \check{C}_{90} are also rather imprecise. Additionally, \check{C}_{90} has the highest error ($E_{90} = 0.1004$ s) among \check{C}_{sp_1} vectors of procedure 5, while \check{C}_{75} along with \check{C}_{85} present the lowest errors $E_{75} \cong E_{85} \cong 0.03$ s. Regarding the indirectly modeled data, in vector \hat{C}_{70} , points 5 to 7 are the least accurate, while in \hat{C}_{80} , the least precise are points 5, 7, and 8. Hence, there are imprecisions when $p_2 = 50\%$ and $p_2 = 70\%$ for both of the sp_1 {70,80} cases.

Procedure 4 presents the higher \bar{E} , as can be seen in Tables 28 and 29. Table 28 shows that vectors \check{C}_{sp_1} for the sp_1 cases {60,65,90} display $E_{sp_1} > 0.1$. Table 29 shows that vector \hat{C}_{80} is more accurate than \hat{C}_{70} , because $E_{80} < E_{70}$ (0.1070 s < 0.1569 s).

With the results presented above, we consider procedures 5 and 6 as the best options for modeling and explaining the observed data. Besides, one important finding is that the pattern of V values, in the range $p_2 = 50\%$ to $p_2 = 80\%$, is not the same among sp_1 cases. It appears that a presence of about 50% of slow vehicles is the lowest threshold from where, and up to 80% in this study, the fast vehicles' extra travel time variability follows a nonlinear pattern.

4.3. Contributions

The contributions of this study are as follows:

A better understanding of the traffic situations recreated through simulations, i.e., situations where vehicles traveling at different speeds interact with each other.

The developed procedures (and models within) for modeling and explaining the observed data from simulations. The best procedures in terms of a lower error were identified.

The patterns of T and V for each sp_1 case and p_2 range were identified. T exhibited an identifiable pattern for all sp_1 cases and p_2 ranges. For all sp_1 cases and the range $p_2 = 10\%$ to 40% , V shows a linear pattern. For sp_1 {60,65,75,80,90} cases and the range $p_2 = 50\%$ to 80% , V shows an unidentifiable pattern. For sp_1 {70} case and the range $p_2 = 50\%$ to 80% , V shows an inverted U-shaped pattern. For sp_1 {85} case and the range $p_2 = 50\%$ to 80% , V shows a U-shaped pattern.

The findings of this work help to better understand heterogeneous traffic scenarios. The procedures can be used to describe the traffic of real locations and, with this information, authorities may decide which actions are required to alleviate traffic issues. Moreover, the traffic outcome of possible future scenarios can help to better plan public infrastructure that avoids congestions, low speeds, high noise levels, pollutions, and other problems that arise as a result of traffic problems.

4.4. Practical Application

A two-lane, one-direction avenue is a common infrastructure in street networks of heterogeneous traffic, i.e., where different types of vehicles circulate and where the vehicles' desired speed may not be the same. Examples of this infrastructure are the avenues' segments described in Table 30.

Table 30. Avenues' features.

Segment' Name	Segment' Location	Start GPS Coordinate	End GPS Coordinate	Segment' Length
Estación Central (north)	Durango, México	24.036787, −104.666690	24.037343, −104.660777	~ 600 m
Estación Central (south)	Durango, México	24.036681, −104.666694	24.037276, −104.660766	~ 600 m

The two segments described in Table 30 are separated by a sidewalk and the posted speed limit for both is 60 km/h, despite that it is common that vehicles traveling at a lower speed than the speed limit slow down the traffic. The procedures introduced in the present study were developed with the intention of analyzing the traffic of segments with similar features to those presented in Table 30. After calibration, the models describe the average extra travel time and the extra travel time variability of the fast vehicles according to the percentage of slow vehicles circulating and the desired speeds. With this information, the corresponding authorities can adjust (or create) policies for restricting or penalizing the slow vehicles in order to keep a desired level of service, or to simply inform users of the current level of service.

5. Conclusions

Procedures 1, 2, and 3 model and explain the mean extra travel time (dependent variable) through the percentage of slow vehicles (independent variable). Procedures 1 and 3 accurately modeled the data for modeling, with procedure 2 being the least accurate. Moreover, procedures 1 and 3 are accurate for explaining the data for validating, both for $p_2 = 10\%$ to 60% , but less accurate for $p_2 = 70\%$ and 80% , concluding that, when the percentage of slow vehicles is 70% or more, it became difficult to explain the data for validating.

Procedures 4, 5, and 6 model and explain the extra travel time variability (dependent variable). In procedure 4, the independent variable is the mean extra travel time, and in procedures 5 and 6, it is the percentage of slow vehicles. Procedure 4 is the least accurate to model the data for modeling and to explain the data for validating, therefore p_2 is a better choice of independent variable than T . Procedures 5 and 6 modeled the data for modeling at approximately equal accuracy. Procedure 5 presents the higher error for \check{C}_{90} , being least precise in the range $p_2 = 40\%$ to 70% . Procedure 6 presents the higher error for \check{C}_{65} , being least precise at $p_2 = 60\%$ and 70% . Moreover, procedures 5 and 6 explain with approximately the same accuracy the data for validating. For procedures 5 and 6, we can say that, in \hat{C}_{70} and \hat{C}_{80} , in the range $p_2 = 10\%$ to 40% , the V values (the corresponding observed values present a linear pattern) in general are better explained than in the range $p_2 = 50\%$ to 80% , although in the last range with $sp_1 = 70$ km/h, the observed V values likely present an inverted U-shaped form, and with $sp_1 = 85$ km/h, a U-shaped form.

Supplementary Materials: The following supporting information can be downloaded at <https://www.mdpi.com/article/10.3390/app12147176/s1>. The name of a folder corresponds with the sp_1 value, a file is named x_y , where x is the p_1 value and y is the p_2 value. For any file, each 8 rows represent the full data of a single vehicle. For any row, we write data each time that a vehicle has traveled a distance $\geq x$, with x taking values from the set $\{20, 40, 60 \dots 500\}$, so we have 25 columns for row. Then, for each 8 rows, we have that the first row is the current time, second is the difference between the current and previous vehicle position, third is the difference between the current and previous time, fourth is the time that a vehicle spend in the left lane between the current and previous time, fifth is the time that a vehicle spend in the right lane between the current and previous time, sixth set to 1 if at the current time the vehicle is in the left lane and set to 0 if it is in the right lane, seventh set to 1 if at the current time the vehicle is in a different lane that at the previous time and set to 0 if it is in the same lane, and eighth the vehicles' speed tendency (sp_1 or sp_2).

Author Contributions: Conceptualization, J.G.C.-G.; methodology, J.G.C.-G.; software, J.G.C.-G.; validation, J.G.C.-G.; formal analysis, J.G.C.-G.; investigation, J.G.C.-G.; resources, J.G.C.-G.; data curation, J.G.C.-G.; writing—original draft preparation, F.P.-M.; writing—review and editing, F.P.-M.; visualization, F.P.-M.; supervision, F.P.-M.; project administration, F.P.-M. All authors have read and agreed to the published version of the manuscript.

Funding: This research received no external funding.

Institutional Review Board Statement: Not applicable.

Informed Consent Statement: Not applicable.

Data Availability Statement: The data presented in this study are available in Supplementary Material.

Conflicts of Interest: The authors declare no conflict of interest.

References

1. Tomtom Traffic Index. Available online: https://www.tomtom.com/en_gb/traffic-index/ranking/ (accessed on 16 August 2020).
2. Carrillo-Gonzalez, J.G.; Lopez-Ortega, J.; Sandoval-Gutierrez, J.; Perez-Martinez, F. Impact of Buses, Taxis, Passenger Cars, and Traffic Infrastructure on Average Travel Speed. *J. Adv. Transp.* **2021**, *2021*, 10. (In English) [CrossRef]
3. Garber, N.J.; Gadiraju, R. Factors affecting speed variance and its influence on accidents. *Transp. Res. Rec.* **1989**, *1213*, 64–71.
4. Kim, J.; Elefteriadou, L. Estimation of Capacity of Two-Lane Two-Way Highways Using Simulation Model. *J. Transp. Eng.* **2010**, *136*, 61–66. (In English) [CrossRef]
5. Moridpour, S.; Mazloumi, E.; Mesbah, M. Impact of heavy vehicles on surrounding traffic characteristics. *J. Adv. Transp.* **2015**, *49*, 535–552. (In English) [CrossRef]
6. Russo, B.J.; Savolainen, P.T.; Gates, T.J.; Kay, J.J.; Frazier, S. Driver speed selection on high-speed two-lane highways: Comparing speed profiles between uniform and differential speed limits. *Traffic Inj. Prev.* **2017**, *18*, 521–527. (In English) [CrossRef]
7. Ghods, A.H.; Saccomanno, F.F. Safety and Traffic Implications of Differential Car and Truck Speed Controls for Two-Lane Highways. *J. Transp. Eng.* **2016**, *142*, 13. (In English) [CrossRef]
8. Russo, B.J.; Rista, E.; Savolainen, P.T.; Gates, T.J.; Frazier, S. Vehicle Speed Characteristics in States with Uniform and Differential Speed Limit Policies Comparative Analysis. *Transp. Res. Rec.* **2015**, *2492*, 1–9. (In English) [CrossRef]
9. Ye, Q.; Tarko, A.P.; Sinha, K.C. A free-flow speed model for Indiana arterial roads. In Proceedings of the 80th Annual Meeting of the Transportation Research Board, Washington, DC, USA, 7–11 January 2001.
10. Medina, A.M.F.; Tarko, A.P. Speed factors on two-lane rural highways in free-flow conditions. *Transp. Res. Rec.* **2005**, *1912*, 39–46. [CrossRef]
11. Deardoff, M.D.; Wiesner, B.N.; Fazio, J. Estimating Free-flow Speed from Posted Speed Limit Signs. In Proceedings of the 6th International Symposium on Highway Capacity and Quality of Service, Stockholm, Sweden, 28 June–1 July 2011; Volume 16, p. 11. (In English) [CrossRef]
12. Hu, W. Raising the speed limit from 75 to 80 mph on Utah rural interstates: Effects on vehicle speeds and speed variance. *J. Saf. Res.* **2017**, *61*, 83–92. (In English) [CrossRef]
13. Kweon, Y.-J.; Kockelman, K.M. Safety effects of speed limit changes: Use of panel models, including speed, use, and design variables. *Transp. Res. Rec.* **2005**, *1908*, 148–158. [CrossRef]
14. Yang, H.; Ye, H.B.; Li, X.W.; Zhao, B.Q. Speed limits, speed selection and network equilibrium. *Transp. Res. Part C Emerg. Technol.* **2015**, *51*, 260–273. (In English) [CrossRef]
15. Barjonet, P.-E. *Traffic Psychology Today*; Springer Science & Business Media: Berlin/Heidelberg, Germany, 2001.
16. Wallén Warner, H. Factors Influencing Drivers' Speeding Behaviour. Ph.D. Thesis, Department of Psychology, Uppsala University, Uppsala, Sweden, 2006. Available online: <https://www.diva-portal.org/smash/record.jsf?pid=diva2%3A169263&dswid=-393> (accessed on 29 January 2021).
17. Wasielewski, P. Speed as a measure of driver risk: Observed speeds versus driver and vehicle characteristics. *Accid. Anal. Prev.* **1984**, *16*, 89–103. (In English) [CrossRef]
18. Haglund, M.; Åberg, L. Stability in drivers' speed choice. *Transp. Res. Part F Traffic Psychol. Behav.* **2002**, *5*, 177–188. [CrossRef]
19. Zaidel, D.M. A modeling perspective on the culture of driving. *Accid. Anal. Prev.* **1992**, *24*, 585–597. (In English) [CrossRef]
20. Rothengatter, T. Risk and the absence of pleasure: A motivational approach to modelling road user behaviour. *Ergonomics* **1988**, *31*, 599–607. (In English) [CrossRef]
21. Connolly, T.; Åberg, L. Some contagion models of speeding. *Accid. Anal. Prev.* **1993**, *25*, 57–66. (In English) [CrossRef]
22. Åberg, L.; Larsen, L.; Glad, A.; Beilinson, L. Observed vehicle speed and drivers' perceived speed of others. *Appl. Psychol. Int. Rev.* **1997**, *46*, 287–302. (In English) [CrossRef]
23. Mahmud, S.M.S.; Ferreira, L.; Hoque, M.S.; Tavassoli, A. Micro Level Speed Choice Behavior on a Rural Highway in an Heterogeneous Traffic Environment: Latent Class Modeling Approach. *Transp. Res. Rec.* **2020**, *2674*, 96–110. (In English) [CrossRef]

24. Tarris, J.P.; Poe, C.M.; Mason, J.M., Jr.; Goulias, K.G. Predicting operating speeds on low-speed urban streets: Regression and panel analysis approaches. *Transp. Res. Rec.* **1996**, *1523*, 46–54. [[CrossRef](#)]
25. Balakrishnan, S.; Sivanandan, R. Influence of lane and vehicle subclass on free-flow speeds for urban roads in heterogeneous traffic. In Proceedings of the 18th Euro Working Group on Transportation, Ewgt 2015, Delft, The Netherlands, 14–16 July 2015; Volume 10, pp. 166–175. (In English) [[CrossRef](#)]
26. Thomas, J.; Srinivasan, K.K.; Arasan, V.T. Vehicle class wise speed-volume models for heterogeneous traffic. *Transport* **2012**, *27*, 206–217. (In English) [[CrossRef](#)]
27. Saha, P.; Roy, N.; Mukherjee, D.; Sarkar, A.K. Application of Principal Component Analysis for Outlier Detection in Heterogeneous Traffic Data. In Proceedings of the 7th International Conference on Ambient Systems, Networks and Technologies (Ant 2016)/the 6th International Conference on Sustainable Energy Information Technology (Seit-2016)/Affiliated Workshops, Madrid, Spain, 23–26 May 2016; Volume 83, pp. 107–114. (In English) [[CrossRef](#)]
28. Al-Kaisy, A.; Durbin, C. Evaluating new methodologies for estimating performance on two-lane highways. *Can. J. Civ. Eng.* **2008**, *35*, 777–785. (In English) [[CrossRef](#)]
29. Rudjito, D. *The Application of Fuzzy Logic to Traffic Assignment in Developing Countries*; Department of Civil and Environmental Engineering, Imperial College London: London, UK, 2007.
30. Chowdhury, D.; Wolf, D.E.; Schreckenberg, M. Particle hopping models for two-lane traffic with two kinds of vehicles: Effects of lane-changing rules. *Phys. A Stat. Mech. Appl.* **1997**, *235*, 417–439. (In English) [[CrossRef](#)]
31. Mallikarjuna, C.; Rao, K.R. Cellular Automata Model for Heterogeneous Traffic. *J. Adv. Transp.* **2009**, *43*, 321–345. (In English) [[CrossRef](#)]
32. Knospe, W.; Santen, L.; Schadschneider, A.; Schreckenberg, M. Disorder effects in cellular automata for two-lane traffic. *Phys. A Stat Mech. Appl.* **1999**, *265*, 614–633. (In English) [[CrossRef](#)]
33. Wong, G.C.K.; Wong, S.C. A multi-class traffic flow model—An extension of LWR model with heterogeneous drivers. *Transp. Res. Part A Policy Pract.* **2002**, *36*, 827–841. (In English) [[CrossRef](#)]
34. Ngoduy, D.; Liu, R. Multiclass first-order simulation model to explain non-linear traffic phenomena. *Phys. A Stat. Mech. Appl.* **2007**, *385*, 667–682. (In English) [[CrossRef](#)]
35. Dey, P.P.; Chandra, S.; Gangopadhyay, S. Simulation of mixed traffic flow on two-lane roads. *J. Transp. Eng.* **2008**, *134*, 361–369. (In English) [[CrossRef](#)]
36. Nair, D.; Yerragunta, S.; Kandaswamy, S.; Venkataraman, H. Assessing the impact of heterogeneous traffic on highways via agent-based simulations. In Proceedings of the Winter Simulation Conference, New York, NY, USA, 14–18 December 2020; pp. 111–122. [[CrossRef](#)]
37. Li, R.; Rose, G.; Sarvi, M. Using automatic vehicle identification data to gain insight into travel time variability and its causes. *Traffic Urban Data* **2006**, 24–32. (In English) [[CrossRef](#)]